Local interactions and their group-level consequences in flocking jackdaws

Hangjian Ling[1], Guillam E. McIvor[2], Kasper van der Vaart[1], Richard T. Vaughan[3], Alex Thornton[2], Nicholas T. Ouellette[1]

[1]Department of Civil and Environmental Engineering, Stanford University, Stanford, CA USA;
[2]Center for Ecology and Conservation, University of Exeter, Penryn, UK;
[3]School of Computing Science, Simon Fraser University, Burnaby, Canada

Correspondence:
Alex Thornton, Email: alex.thornton@exeter.ac.uk
Nicholas T. Ouellette, Email: nto@stanford.edu

Abstract: As one of nature's most striking examples of collective behaviour, bird flocks have attracted extensive research. However, we still lack an understanding of the attractive and repulsive forces that govern interactions between individuals within flocks and how these forces influence neighbours' relative positions and ultimately determine the shape of flocks. We address these issues by analysing the three-dimensional movements of wild jackdaws (*Corvus monedula*) in flocks containing 2 to 338 individuals. We quantify the social interaction forces in large, airborne flocks and find that these forces are highly anisotropic. The long-range attraction in the direction perpendicular to the movement direction is stronger than that along it, and the short-range repulsion is generated mainly by turning rather than changing speed. We explain this phenomenon by considering the wingbeat frequency and the change in the kinetic and gravitational potential energy during flight, and find that changing the direction of movement is less energetically costly than adjusting speed for birds. Furthermore, our data show that collision avoidance by turning can alter local neighbour distributions and ultimately change the group shape. Our results illustrate the macroscopic consequences of anisotropic interaction forces in bird flocks, and help to draw links between group structure, local interactions, and the biophysics of animal locomotion.

Key words: Collective behaviour; Flocking; Social interactions; Biophysics of locomotion; Corvids; 3D imaging

1. Introduction

Highly coordinated collective motion is a cornerstone of many biological systems at all scales, from cell colonies [1,2] to insect swarms [3–6], fish schools [7,8], bird flocks [9–11], ungulate herds [12–14], and even human crowds [15,16]. Moving together in large groups and using social information can provide numerous benefits, including enhanced predator avoidance [17–19], more efficient resource exploitation [20,21], energy savings [22–24] and efficient learning of migration routes [25,26]. Thus, understanding the mechanisms driving the emergence of collectivity in natural systems has significant ecological, evolutionary, and cognitive implications [27]. Over the past few decades, theoretical models [28–37] have demonstrated that global-level collective motion can be generated by simple local interactions. However, verification of these interaction rules using data from real moving animals has lagged behind due to measurement challenges. Now that new measurement technologies have made it more feasible to track animal movement, characterizing the local interactions in animal groups in natural environments is critical for advancing our understanding of collective behaviour [38,39].

Bird flocks are one of the most striking and frequently studied examples of collective behaviour. They are often modelled using agent-based frameworks [40–42] where individuals follow simple interaction rules such as long-range attraction, short-range repulsion, and intermediate-range alignment. These interactions are treated as social “forces” [43] imposed by the presence of nearby neighbours that thus determine the acceleration of each agent. Although many empirical measurements of bird flocks have been made [44,45,54–56,46–53], the fundamental interaction rules assumed in the models have still not been fully tested. In particular, the effective attractive and repulsive forces that birds experience while flying in large flocks has not been studied. It thus remains unclear how interaction forces vary depending on the relative positions of neighbouring individuals. Characterizing such interaction forces is, however, critical for

understanding the flock mechanics, since the forces acting on individuals will determine their velocities, relative positions in the group, and ultimately the shape of the entire group [42,44]. Moreover, from an adaptive perspective, the morphology of animal groups and the distribution of individuals within them influences group members' access to social information and vulnerability to predation [42,57–59].

One way to infer the effective attractive and repulsive forces between group members is by analysing the accelerations of individuals [60,61], since forces are proportional to accelerations. Based on this idea, Katz *et al.* (2011) [60] used optical tracking to measure the acceleration of individuals as a function of the distance to neighbours (known as a "force map") in schools of two or three captive fish, finding evidence for both long-range attraction and short-range repulsion. Similarly, by fitting observational data to a zonal model [43] where individuals' accelerations are explicitly related to the interaction forces, Lukeman et al. (2010) [50] found long-range attraction and short-range repulsion in large flocks of sea ducks (surf scoters) congregated on the surface of the sea. In airborne flocks, the only study of forces to date [44] reported force maps for isolated pairs of homing pigeons based on GPS (Global Positioning System) tracking, though the measured forces had large uncertainties, with a position uncertainty of more than two times the bird body size. Thus, well-resolved force maps similar to those measured in fish schools are currently unavailable for bird flocks in flight. More generally, given the reliance of previous research on small groups of (often captive) animals, the interaction forces at play in large, natural collective aggregations such as aerial bird flocks remain unknown. Since birds interact with more than one other individual in large groups [48,55], the forces measured in isolated pairs may not be representative of how birds interact in large flocks.

Current research also tells us little about the mechanisms governing the side-by-side neighbour structure seen in flocks of small birds (e.g. pigeons, starlings or jackdaws) [44,48,49,55], which in turn may determine the overall shape of flocks. One hypothesis, proposed in previous studies [44,62], is that the mechanism of short-range repulsion determines the local neighbour distribution. This hypothesis is illustrated in figure 1: avoiding collisions by changing speed (*speeding-based* repulsion) is thought to lead to a front-to-back distribution, while avoiding collisions by turning (*turning-based* repulsion) should result in a side-by-side structure [42]. This hypothesis has been verified in small groups of fish that use *speeding-based* repulsion [60,62,63], and by pigeons in groups of two that use *turning-based* repulsion [44]. However, it is not known whether birds in large groups avoid collisions by turning. Therefore, whether this hypothesis explains the side-by-side neighbour structure observed in large bird flocks has yet to be tested.

Moreover, the reason why birds flying in small groups prefer to use *turning-based* repulsion, as reported in a previous study [44], is not fully understood. Previous researchers [38,44] have suggested that the cause is due to the relative ease of turning as opposed to changing speed when flying through a low-density fluid like air and contrasted this with schools of fish moving in denser water, where changes in speed seem to be simpler [60,62–64]. This argument is reasonable, since flight speed is directly related to power consumption for flapping flight [65,66]. However, the energetic cost difference between making turns and changing speed has not been examined for birds flying in flocks. Whether turning is easier than changing speed and thus the ultimate cause of birds' use of *turning-based* repulsion is unclear.

Finally, it remains unclear how the positions of neighbours determine the overall shape of flocks. In fish schools, there is evidence that the local structure scales up to the school level, leading the entire group to be elongated along the movement direction [62,64]. In contrast, the group-

level consequences of the side-by-side local structure typical of many bird flocks have yet to be examined. Consequently, we lack an understanding of the connection between individual interaction forces, local neighbour structures, and the overall shape of flocks.

Here, we address these open questions using jackdaws (*Corvus monedula*), a small corvid species, as a model system. Jackdaws are an excellent system for testing movement interactions since they are highly social on several levels [67]. They form long-term monogamous pair bonds, and bonded pairs frequently fly together, but they also fly in large groups of up to thousands of individuals during the winter roosting season [68]. Flock flight paths are very predictable, allowing us to measure the three-dimensional (3D) trajectories of individuals in these flocks using a ground-based stereo-imaging system [56]. Our uncertainty in the measurement of bird position is about 0.04 m—much smaller than both the body size of a jackdaw (0.3-0.4 m) and substantially lower than in previous studies [44]—allowing very accurate acceleration measurements. Using these measurements, we are able to construct well-resolved force maps and test for the existence of long-range attraction and short-range repulsion in both isolated pairs and large flocks. We confirm that birds modulate their distance to nearby neighbours primarily by turning rather than changing speed even in large flocks, and therefore explain the side-by-side neighbour distribution. By measuring the wingbeat frequency, we provide evidence that the dominance of turning-based interactions is likely due to the biophysics of bird locomotion, as turning is energetically cheaper than changing speed. Finally, we show that the side-by-side local structure does indeed scale up to the flock level, leading to flocks that are elongated transverse to the direction of motion. These results give a more firm foundation for the structure of local interactions in bird flocks, which can be used to develop more accurate theoretical models.

2. Materials and Methods

(a) Data collection

We used a stereo-imaging system to measure the three-dimensional (3D) trajectories of each individual bird within both isolated pairs and large flocks. The system used four synchronised, high-speed USB-3 cameras (Basler ace acA2040-90um, pixel size of 5.5 μm, sensor resolution of 2048 by 2048 pixels) with overlapping fields of view. We placed the imaging system along the typical flight paths of flocks such that the birds flew directly over the camera array. The maximal distance between cameras was between 50 and 60 m, which was on the same order of the distance from the camera to the birds (~50 m). At a height of 50 m, we were able to image an area of 60 by 60 m^2 and determine bird positions with an uncertainty of 0.04 m—much smaller than the jackdaw body length (0.3~0.4 m). We recorded the birds' movement continuously for 3 to 20 seconds at 60 fps. Each flocking event consisted of 180 to 1200 frames. The imaging locations were in the vicinity of winter roosts near Mabe and Gwennap, Cornwall, UK. More details of the stereo-imaging system can be found in Ling *et al*. (2018) [56]. The camera calibration procedure can be found in the *electronic supplementary material*.

After recording the image data, we reconstructed the trajectories of individual birds in 3D space (details of the 3D reconstruction and tracking procedures can be found in the *electronic supplementary material)*. Along each bird's trajectory, we measured the position x_i, velocity v_i, and acceleration a_i corresponding to the bird bodies in a Cartesian coordinate system, where i ranges from 1 to 3. The direction of gravity was aligned to $-x_3$. We use $\boldsymbol{x}$, $\boldsymbol{v}$, and $\boldsymbol{a}$ to denote the vectors of the corresponding quantities, and t to denote time. Moreover, following our previous studies [55,56], we measured the time series of wingbeat frequency along each bird's trajectory, denoted as f_{wb} (see *electronic supplementary material*). We also measured the total energy of birds as $E=0.5|\boldsymbol{v}|^2+gx_3$, where g=9.8 m/s^2 is the gravitational acceleration. We defined the rate of change of E as $E'=(E(t+dt)-E(t))/dt$, where dt is the time step. $E'>0$ indicates an increase of power output, assuming a constant drag force.

(b) Flocking events

We recorded a number of flocking events from December 2017 to March 2018. The events included groups consisting of as few as two to as many as several hundred individuals. We defined two birds to be an isolated pair if (i) the two birds were not in a large group and (ii) the distance to the closest third bird was larger than 20 m, five times the average distance separating a pair of birds. We obtained 305 isolated pairs of jackdaws with mean trajectory length of 4.0 s. Recorded bird images and reconstructed 3D trajectories for a sample isolated pair are shown in figure 2a-c. More samples are shown in *electronic supplementary material figure S1*.

We also recorded six flocks, which we label #1 to #6, consisting of 26 to 338 jackdaws. Criteria for the selection of flocking events are provided in the *electronic supplementary material*. Recorded bird images and reconstructed 3D trajectories for flock #1 are shown in figure 3a-c. Trajectories for flocks #2 to #6 are shown in *electronic supplementary material figure S2*. Statistics of the distance to nearest neighbours, flight speed, and acceleration are listed in Table 1. Since the flight speed was primarily in the horizontal plane ($v_3 << |\boldsymbol{v}|$), we neglect the component in the gravity direction in the following analysis.

(c) Data analysis

As shown in figures 2 and 3, both speed and movement direction varied both in time and between different birds. To understand how birds adjust their velocity, we adopt the force-based approach used by Katz *et al*. (2011) [60]. We approximate the attraction or repulsion force $\boldsymbol{F}$ of a focal bird in response to a neighbouring bird by measuring the relative acceleration between the two, so that $\boldsymbol{F} = \boldsymbol{a}^{\text{focal}} - \boldsymbol{a}^{\text{neighbour}}$, where the superscripts '*focal*' and '*neighbour'* denote quantities measured for the focal and neighbour birds, respectively. We subtracted the neighbour

188 acceleration $\boldsymbol{a}^{\text{neighbour}}$ in order to remove the environmental effects acting similarly on both birds.
189 For example, when both birds are linearly accelerating, $\boldsymbol{a}^{\text{focal}}$ can be very large but does not
190 represent the force due to the neighbour. Only the relative quantity $\boldsymbol{F}$ captures the interaction
191 between two birds.
192
193 Using the local coordinate system sketched in figure 4(a), we decompose $\boldsymbol{F}$ into two
194 components: one projected in the movement direction of focal birds that we denote as a
195 'speeding force' F_{Speed}, and one projected perpendicular to the flight direction that we denote as
196 a 'turning force' F_{Turn}. Therefore, positive (negative) F_{Speed} implies speeding up (slowing down),
197 and positive (negative) F_{Turn} implies turning right (left). For simplicity, we will call the direction
198 perpendicular to the movement direction the *wing direction*. We label distances in the wing
199 direction as d_{Wing} and distances in the movement direction as d_{Move}. Therefore, positive (negative)
200 d_{Wing} values mean that a neighbouring bird is located on the right (left), and positive (negative)
201 d_{Move} values mean that a neighbouring bird is located in the front (back). The details of our
202 calculation of two-dimensional force maps and one-dimensional force curves are described in
203 the *electronic supplementary material*.
204
205 **3. Results**
206 (a) Interaction forces
207 In isolated pairs, the turning force (F_{Turn}) strongly depends on d_{Wing} and is relatively insensitive to
208 d_{Move} (figure 4b). When plotting F_{Turn} as a function of d_{Wing} (figure 4d), long-range attraction
209 zones where the focal bird turned right (left) when a neighbour was far on the right (left) and
210 short-range repulsion zones where the focal bird turned left (right) when a neighbour was just on
211 the right (left) are clearly evident. F_{Turn} switches from repulsive to attractive at $|d_{Wing}|$=0.9 m (≈2.5
212 jackdaw body lengths). Conversely, the speeding force (F_{Speed}) strongly depends on d_{Move} and is

insensitive to d_{Wing} (figure 4c). Plotting F_{Speed} as a function of d_{Move} (figure 4d) reveals attraction zones where the focal bird slowed down (sped up) when a neighbour was in back (front), but no repulsion zones. The observation that repulsion is only present in the map of the turning force indicates that birds avoid collisions mainly by turning. Moreover, the magnitude of the turning force is about twice as large as the speeding force in the attraction zone. The anisotropy of the force in the wing and movement directions is consistent with the observation that the standard deviation of $\boldsymbol{a}$ in the wing direction was larger than that in the movement direction (Table 1). We also find that $|F_{Speed}|$ increases with the flight speed of focal birds, similar to fish [60], while $|F_{Turn}|$ does not show a clear relationship with speed (*electronic supplementary material figure S3*).

When flying in large flocks (flocks #1 to #6), the anisotropy of attraction and repulsion in the wing and movement directions persists, with the absolute value of the turning forces larger than that of the speeding forces and with repulsion governed by turning (figure 5). Note that the anisotropy was independent of whether the entire group was making small turns (flock #1, where $\boldsymbol{a}$ in the wing direction was larger than in the movement direction) or changing speed (flocks #2 to #6 where $\boldsymbol{a}$ in the movement direction was larger than in the wing direction). The results are also consistent for flock sizes ranging from 26 to 338 individuals (figure 5; Table 1).

(b) Neighbour structure and group shape

For both isolated pairs (figure 6a) and large flocks (figure 6b, *electronic supplementary material figure S4*), we find that birds prefer to fly side by side, in that the most probable location for a neighbouring bird was at d_{Wing}=1.0 m (≈2.8 jackdaw body lengths) and d_{Move}=0. In a previous study [55], we found that these anisotropic spatial distributions of neighbours become isotropic for large topological distance (as in starlings [48]), a feature that we used to estimate the interaction range. We found that birds not part of a bonded pair typically interacted with 7 to 8 neighbours [55].

We then examined whether this local anisotropic structure scales up and causes the overall shape of the flock to be elongated. As shown in figure 6(c) and *electronic supplementary material figure S5*, entire flocks typically appear to consist of several distinguishable subgroups separated along the movement direction. We thus partitioned each flock into N_s subgroups using *k*-means clustering, where N_s was the number of distinguishable peaks in the distribution of bird positions along the flight direction (figure 6(d), *electronic supplementary material figure S5*). We considered the largest subgroup in each flock and calculated its extent in the movement and wing directions, which we label as L_{Move} and L_{Wing}, respectively. We find that all subgroups are elongated in the wing direction (figure 6e), indicating that the side-by-side local structure does indeed percolate upscale and has group-level consequences. The generation of multiple subgroups along the movement direction is likely due to weaker attractive forces in that direction compared to the wing direction (figure 5). The flocks as a whole are however still elongated in the wing direction (*electronic supplementary material figure S6*), though with a smaller L_{Wing}/L_{Move} as compared to subgroups.

(c) Wingbeat frequency and flight power output

To understand why birds avoid collision mainly by turning instead of changing speed, we examined the dependence of $df_{wb} = f_{wb}^{focal} - f_{wb}^{neighbour}$ as a function of d_{Wing} and d_{Move}, as shown in figure 7(a) and (b), respectively. We also studied the dependence of $dE' = E'^{\,focal} - E'^{\,neighbour}$ on d_{Wing} and d_{Move}, as shown in figure 7(c) and (d), respectively. Both df_{wb} and dE' are close to zero for all values of d_{Wing}, indicating that turning towards a neighbouring bird does not require a change of wingbeat frequency and power output. However, df_{wb} is up to 10% of the mean wingbeat frequency for large d_{Move} and dE' increases linearly with d_{Move}, indicating that focal birds must increase their wingbeat frequency and power output to achieve a positive speeding force when the neighbouring bird is far to the front. Our results suggest that turning is

energetically cheaper than changing speed, and thus provide a possible explanation for the turning-based repulsion used by birds. Additionally, comparing between rear and front birds in isolated pairs shows that rear birds are more likely to change their behaviour (e.g., to generate positive speeding forces, rear birds are more likely to increase their wingbeat frequency and speed up) in response to front birds (see details in *electronic supplementary material*).

4. Discussion

Characterizing the social interactions in large groups of birds is critical for understanding the mechanisms of flocking behaviour. Here, by measuring the acceleration of a focal bird in response to its neighbours, we quantified the social interaction forces in groups with sizes ranging from two to hundreds of individuals. Our measurements of short-range repulsion and long-range attraction in bird flocks agree with agent-based models [29–34,40,41,59] and empirical measurements in insects [61,69,70], fish [8,60,71], birds [44,50] and mammals [72]. Moreover, we find that the effective attraction force (that is, the magnitude of the acceleration) increases linearly with distance in a spring-like fashion, consistent with assumptions made in theoretical models [33,34] and observational results from fish schools [60]. Critically, our analyses reveal that the social forces are highly anisotropic: long-range attractive forces are larger in the wing direction than in the movement direction, and short-range repulsive forces are generated mainly by turning. Although similarly anisotropic forces have been reported previously for pairs of pigeons [44], we show here that this effect extends to large flocks.

Thus, we also provide empirical support for the hypothesis [44,62] that the side-by-side neighbour structures typical of pigeon and passerine bird flocks [44,48,49,55] are a result of the turning-based repulsion mechanism. As shown in previous studies [10,55,56], both jackdaws and pigeons flying in side-by-side configurations in large flocks expend more energy than they do when flying alone. Therefore, the side-by-side neighbour structure is unlikely to arise from

291 aerodynamic interactions, in contrast with V-formation flight of some waterfowl and large
292 migratory birds [22,23,73].
293
294 Furthermore, by measuring the wingbeat frequency and the sum of the potential and kinetic
295 energy during flight for birds in isolated pairs, we give an explanation for why birds use turning-
296 based repulsion rather than the speeding-based repulsion seen in fish schools [60,62]. We find
297 that generating large speeding forces requires birds to change their wingbeat frequency and
298 power output, while producing a large turning force does not. Our results suggest that turning is
299 likely to be energetically cheaper then changing speed. This observation can be explained by
300 the physics of bird locomotion: as they travel through the air, birds have to maintain sufficient
301 speed to gain enough lift force and minimize the mechanical power output [65] (since both
302 increasing and reducing speeds may result in an increase of power output). On the other hand,
303 since the drag force in air is relatively small due to its low density, slightly adjusting the flight
304 direction (by, e.g., changing body posture [74,75]) will not cause a significant change of speed
305 and thus will require little additional power output. Therefore, it is likely that the physics of bird
306 locomotion make turning easier and energetically cheaper than changing speed, resulting in
307 dominantly turning-based repulsion, in contrast to the changes in speed that control repulsion in
308 fish moving through the higher density medium of water [60,62,63].
309
310 Finally, we demonstrate that the local side-by-side structure scales up to the global level,
311 making the entire flock elongated in the direction perpendicular to the movement. This is similar
312 to the way in which fish schools are elongated in the movement direction as a result of the front-
313 to-back local configuration of neighbours [42,62–64]. We note, however, that the elongated
314 group shape was observed here for birds traveling together in a particular direction (in this case,
315 towards evening roosts). Display flocks that make more complex manoeuvres (such as the
316 classic murmurations of starlings) may show different behaviour. For example, when a group of

starlings makes a turn, it was found that the group was initially elongated along the direction perpendicular to the movement before the turn but became elongated along the traveling direction after the turn [49].

In conclusion, although many previous models have assumed that interaction forces depend only on the distance between neighbours, we show that due to the physics of bird locomotion (and in particular that turning is easier than changing speed), the social interaction forces in real animal groups are highly anisotropic. Such anisotropic forces have significant consequences both for the local neighbour structure and the macroscopic group shapes, which ultimately impact key functions such as information transfer [64] and predator avoidance [18]. We thus strongly suggest that future models should consider the physics of animal locomotion and the properties of the medium through which animals are traveling when formulating interaction rules.

Ethical note

All field protocols were approved by the Biosciences Ethics Panel of the University of Exeter (ref 2017/2080) and adhered to the Association for the Study of Animal Behaviour Guidelines for the Treatment of Animals in Behavioural Research and Teaching.

Data accessibility

Data and code are available from the Dryad Digital Repository at: https://datadryad.org/review?doi=doi:10.5061/dryad.kb8js06 [76].

Competing interests

We declare we have no competing interests.

Authors' contributions

H.L., N.T.O, A.T., and R.T.V. conceived the ideas; H.L. and N.T.O. designed the methodology; G.E.M. and A.T. collected the data; H.L., N.T.O, and K.V. analysed the data; All led the writing of the manuscript. All authors contributed critically to the drafts and gave final approval for publication.

Acknowledgements

We are grateful to Paul Dunstan, Richard Stone, and the Gluyas family for permission to work on their land, and to Victoria Lee, Beki Hooper, Amy Hall, Paige Petts, Christoph Petersen, and Joe Westley for their assistance in the field.

Funding

This work was supported by a Human Frontier Science Program grant to AT, NTO and RTV, Award Number RG0049/2017.

References

1. Lushi E, Wioland H, Goldstein RE. 2014 Fluid flows created by swimming bacteria drive self-organization in confined suspensions. *Proc. Natl. Acad. Sci.* **111**, 9733–9738. (doi:10.1073/pnas.1405698111)
2. Chen X, Dong X, Be'Er A, Swinney HL, Zhang HP. 2012 Scale-invariant correlations in dynamic bacterial clusters. *Phys. Rev. Lett.* **108**, 148101. (doi:10.1103/PhysRevLett.108.148101)
3. Sinhuber M, Ouellette NT. 2017 Phase Coexistence in Insect Swarms. *Phys. Rev. Lett.* **119**, 178003. (doi:10.1103/PhysRevLett.119.178003)
4. Cavagna A, Conti D, Creato C, Del Castello L, Giardina I, Grigera TS, Melillo S, Parisi L,

Viale M. 2017 Dynamic scaling in natural swarms. *Nat. Phys.* **13**, 914–918. (doi:10.1038/nphys4153)

5. Attanasi A *et al.* 2014 Collective Behaviour without Collective Order in Wild Swarms of Midges. *PLoS Comput. Biol.* **10**, e1003697. (doi:10.1371/journal.pcbi.1003697)

6. Méndez-Valderrama JF, Kinkhabwala YA, Silver J, Cohen I, Arias TA. 2018 Density-functional fluctuation theory of crowds. *Nat. Commun.* **9**. (doi:10.1038/s41467-018-05750-z)

7. Jolles JW, Boogert NJ, Sridhar VH, Couzin ID, Manica A. 2017 Consistent Individual Differences Drive Collective Behavior and Group Functioning of Schooling Fish. *Curr. Biol.* **27**, 2862-2868.e7. (doi:10.1016/j.cub.2017.08.004)

8. Hinz RC, de Polavieja GG. 2017 Ontogeny of collective behavior reveals a simple attraction rule. *Proc. Natl. Acad. Sci.* **114**, 2295–2300. (doi:10.1073/pnas.1616926114)

9. Sasaki T, Mann RP, Warren KN, Herbert T, Wilson T, Biro D. 2018 Personality and the collective: bold homing pigeons occupy higher leadership ranks in flocks. *Philos. Trans. R. Soc. B Biol. Sci.* **373**, 20170038. (doi:10.1098/rstb.2017.0038)

10. Usherwood JR, Stavrou M, Lowe JC, Roskilly K, Wilson AM. 2011 Flying in a flock comes at a cost in pigeons. *Nature* **474**, 494–497. (doi:10.1038/nature10164)

11. Bajec IL, Heppner FH. 2009 Organized flight in birds. *Anim. Behav.* **78**, 777–789. (doi:10.1016/j.anbehav.2009.07.007)

12. Inoue S, Yamamoto S, Ringhofer M, Mendonça RS, Pereira C, Hirata S. 2018 Spatial positioning of individuals in a group of feral horses: a case study using drone technology. *Mammal Res.* (doi:10.1007/s13364-018-0400-2)

13. Strandburg-Peshkin A, Farine DR, Crofoot MC, Couzin ID. 2017 Habitat and social factors shape individual decisions and emergent group structure during baboon collective movement. *Elife* **6**, e19505. (doi:10.7554/eLife.19505)

14. Strandburg-Peshkin A, Farine DR, Couzin ID, Crofoot MC. 2015 Shared decision-making

drives collective movement in wild baboons. *Science (80-.).* **348**, 1358–1361. (doi:10.1126/science.aaa5099)

15. Silverberg JL, Bierbaum M, Sethna JP, Cohen I. 2013 Collective motion of humans in mosh and circle pits at heavy metal concerts. *Phys. Rev. Lett.* **110**, 1–5. (doi:10.1103/PhysRevLett.110.228701)

16. Moussaïd M, Perozo N, Garnier S, Helbing D, Theraulaz G. 2010 The walking behaviour of pedestrian social groups and its impact on crowd dynamics. *PLoS One* **5**, 1–7. (doi:10.1371/journal.pone.0010047)

17. Ioannou CC, Guttal V, Couzin ID. 2012 Predatory Fish Select for Coordinated Collective Motion in Virtual Prey. *Science (80-.).* **337**, 1212–1215. (doi:10.1126/science.1218919)

18. Handegard NO, Boswell KM, Ioannou CC, Leblanc SP, Tjøstheim DB, Couzin ID. 2012 The Dynamics of Coordinated Group Hunting and Collective Information Transfer among Schooling Prey. *Curr. Biol.* **22**, 1213–1217. (doi:10.1016/j.cub.2012.04.050)

19. Ward AJW, Herbert-Read JE, Sumpter DJT, Krause J. 2011 Fast and accurate decisions through collective vigilance in fish shoals. *Proc. Natl. Acad. Sci.* **108**, 2312–2315. (doi:10.1073/pnas.1007102108)

20. Berdahl A, Torney CJ, Ioannou CC, Faria JJ, Couzin ID. 2013 Emergent Sensing of Complex Environments by Mobile Animal Groups. *Science (80-.).* **339**, 574–576. (doi:10.1126/science.1225883)

21. Hein AM, Rosenthal SB, Hagstrom GI, Berdahl A, Torney CJ, Couzin ID. 2015 The evolution of distributed sensing and collective computation in animal populations. *Elife* **4**, 1–43. (doi:10.7554/eLife.10955)

22. Portugal SJ, Hubel TY, Fritz J, Heese S, Trobe D, Voelkl B, Hailes S, Wilson AM, Usherwood JR. 2014 Upwash exploitation and downwash avoidance by flap phasing in ibis formation flight. *Nature* **505**, 399–402. (doi:10.1038/nature12939)

23. Weimerskirch H, Martin J, Clerquin Y, Alexandre P, Jiraskova S. 2001 Energy saving in

flight formation. *Nature* **413**, 697–698. (doi:10.1038/35099670)

24. Marras S, Killen SS, Lindström J, McKenzie DJ, Steffensen JF, Domenici P. 2015 Fish swimming in schools save energy regardless of their spatial position. *Behav. Ecol. Sociobiol.* **69**, 219–226. (doi:10.1007/s00265-014-1834-4)

25. Mueller T, O'Hara RB, Converse SJ, Urbanek RP, Fagan WF. 2013 Social Learning of Migratory Performance. *Science (80-.).* **341**, 999–1002. (doi:10.1126/science.1237139)

26. Couzin ID. 2018 Collective animal migration. *Curr. Biol.* **28**, R976–R980. (doi:10.1016/j.cub.2018.04.044)

27. King AJ, Fehlmann G, Biro D, Ward AJ, Fürtbauer I. 2018 Re-wilding Collective Behaviour: An Ecological Perspective. *Trends Ecol. Evol.* **33**, 347–357. (doi:10.1016/j.tree.2018.03.004)

28. Vicsek T, Czirók A, Ben-Jacob E, Cohen I, Shochet O. 1995 Novel Type of Phase Transition in a System of Self-Driven Particles. *Phys. Rev. Lett.* **75**, 1226–1229. (doi:10.1103/PhysRevLett.75.1226)

29. Couzin ID, Krause J, James R, Ruxton GD, Franks NR. 2002 Collective Memory and Spatial Sorting in Animal Groups. *J. Theor. Biol.* **218**, 1–11. (doi:10.1006/jtbi.2002.3065)

30. Strömbom D. 2011 Collective motion from local attraction. *J. Theor. Biol.* **283**, 145–151. (doi:10.1016/j.jtbi.2011.05.019)

31. Romanczuk P, Schimansky-Geier L. 2012 Swarming and pattern formation due to selective attraction and repulsion. *Interface Focus* **2**, 746–756. (doi:10.1098/rsfs.2012.0030)

32. Grégoire G, Chaté H. 2004 Onset of Collective and Cohesive Motion. *Phys. Rev. Lett.* **92**, 025702. (doi:10.1103/PhysRevLett.92.025702)

33. Huepe C, Ferrante E, Wenseleers T, Turgut AE. 2015 Scale-Free Correlations in Flocking Systems with Position-Based Interactions. *J. Stat. Phys.* **158**, 549–562. (doi:10.1007/s10955-014-1114-8)

34. Grégoire G, Chaté H, Tu Y. 2003 Moving and staying together without a leader. *Phys. D Nonlinear Phenom.* **181**, 157–170. (doi:10.1016/S0167-2789(03)00102-7)
35. Sumpter DJT. 2006 The principles of collective animal behaviour. *Philos. Trans. R. Soc. B Biol. Sci.* **361**, 5–22. (doi:10.1098/rstb.2005.1733)
36. Vicsek T, Zafeiris A. 2012 Collective motion. *Phys. Rep.* **517**, 71–140. (doi:10.1016/j.physrep.2012.03.004)
37. Bialek W, Cavagna A, Giardina I, Mora T, Silvestri E, Viale M, Walczak AM. 2012 Statistical mechanics for natural flocks of birds. *Proc. Natl. Acad. Sci.* **109**, 4786–4791. (doi:10.1073/pnas.1118633109)
38. Herbert-Read JE. 2016 Understanding how animal groups achieve coordinated movement. *J. Exp. Biol.* **219**, 2971–2983. (doi:10.1242/jeb.129411)
39. Hughey LF, Hein AM, Strandburg-Peshkin A, Jensen FH. 2018 Challenges and solutions for studying collective animal behaviour in the wild. *Philos. Trans. R. Soc. B Biol. Sci.* **373**, 20170005. (doi:10.1098/rstb.2017.0005)
40. Bode NWF, Franks DW, Wood AJ. 2011 Limited interactions in flocks: Relating model simulations to empirical data. *J. R. Soc. Interface* **8**, 301–304. (doi:10.1098/rsif.2010.0397)
41. Hemelrijk CK, Hildenbrandt H. 2011 Some Causes of the Variable Shape of Flocks of Birds. *PLoS One* **6**, e22479. (doi:10.1371/journal.pone.0022479)
42. Hemelrijk CK, Hildenbrandt H. 2012 Schools of fish and flocks of birds: their shape and internal structure by self-organization. *Interface Focus* **2**, 726–737. (doi:10.1098/rsfs.2012.0025)
43. Levine H, Rappel W-J, Cohen I. 2000 Self-organization in systems of self-propelled particles. *Phys. Rev. E* **63**, 017101. (doi:10.1103/PhysRevE.63.017101)
44. Pettit B, Perna A, Biro D, Sumpter DJT. 2013 Interaction rules underlying group decisions in homing pigeons. *J. R. Soc. Interface* **10**. (doi:10.1098/rsif.2013.0529)

45. Chen D, Liu X, Xu B, Zhang H-T. 2017 Intermittence and connectivity of interactions in pigeon flock flights. *Sci. Rep.* **7**, 10452. (doi:10.1038/s41598-017-09986-5)
46. Nagy M, Ákos Z, Biro D, Vicsek T. 2010 Hierarchical group dynamics in pigeon flocks. *Nature* **464**, 890–893. (doi:10.1038/nature08891)
47. Nagy M, Vasarhelyi G, Pettit B, Roberts-Mariani I, Vicsek T, Biro D. 2013 Context-dependent hierarchies in pigeons. *Proc. Natl. Acad. Sci.* **110**, 13049–13054. (doi:10.1073/pnas.1305552110)
48. Ballerini M *et al.* 2008 Interaction ruling animal collective behavior depends on topological rather than metric distance: Evidence from a field study. *Proc. Natl. Acad. Sci.* **105**, 1232–1237. (doi:10.1073/pnas.0711437105)
49. Ballerini M *et al.* 2008 Empirical investigation of starling flocks: a benchmark study in collective animal behaviour. *Anim. Behav.* **76**, 201–215. (doi:10.1016/j.anbehav.2008.02.004)
50. Lukeman R, Li Y-X, Edelstein-Keshet L. 2010 Inferring individual rules from collective behavior. *Proc. Natl. Acad. Sci.* **107**, 12576–12580. (doi:10.1073/pnas.1001763107)
51. Pearce DJG, Miller AM, Rowlands G, Turner MS. 2014 Role of projection in the control of bird flocks. *Proc. Natl. Acad. Sci.* **111**, 10422–10426. (doi:10.1073/pnas.1402202111)
52. Evangelista D, Ray D, Raja S, Hedrick T. 2017 Three-dimensional trajectories and network analyses of group behaviour within chimney swift flocks during approaches to the roost. *Proc R Soc B* **284**, 20162602. (doi:10.1098/rspb.2016.2602)
53. Cavagna A, Cimarelli A, Giardina I, Parisi G, Santagati R, Stefanini F, Viale M. 2010 Scale-free correlations in starling flocks. *Proc. Natl. Acad. Sci.* **107**, 11865–11870. (doi:10.1073/pnas.1005766107)
54. Mora T, Walczak AM, Castello LD, Ginelli F, Melillo S, Parisi L, Viale M, Cavagna A, Giardina I. 2016 Local equilibrium in bird flocks. *Nat Phys* **12**, 1153–1157. (doi:10.1038/nphys3846)

55. Ling H, Mclvor GE, van der Vaart K, Vaughan RT, Thornton A, Ouellette NT. 2019 Costs and benefits of social relationships in the collective motion of bird flocks. *Nat. Ecol. Evol.* (doi:10.1038/s41559-019-0891-5)

56. Ling H, Mclvor GE, Nagy G, MohaimenianPour S, Vaughan RT, Thornton A, Ouellette NT. 2018 Simultaneous measurements of three-dimensional trajectories and wingbeat frequencies of birds in the field. *J. R. Soc. Interface* **15**, 20180653. (doi:10.1098/rsif.2018.0653)

57. Sumpter D, Buhl J, Biro D, Couzin I. 2008 Information transfer in moving animal groups. *Theory Biosci.* **127**, 177–186. (doi:10.1007/s12064-008-0040-1)

58. Fern﷿ndez-Juricic E, Kacelnik A. 2004 Information transfer and gain in flocks: the effects of quality and quantity of social information at different neighbour distances. *Behav. Ecol. Sociobiol.* **55**, 502–511. (doi:10.1007/s00265-003-0698-9)

59. Hogan BG, Hildenbrandt H, Scott-Samuel NE, Cuthill IC, Hemelrijk CK. 2017 The confusion effect when attacking simulated three-dimensional starling flocks. *R. Soc. Open Sci.* **4**, 160564. (doi:10.1098/rsos.160564)

60. Katz Y, Tunstrom K, Ioannou CC, Huepe C, Couzin ID. 2011 Inferring the structure and dynamics of interactions in schooling fish. *Proc. Natl. Acad. Sci.* **108**, 18720–18725. (doi:10.1073/pnas.1107583108)

61. Puckett JG, Kelley DH, Ouellette NT. 2015 Searching for effective forces in laboratory insect swarms. *Sci. Rep.* **4**, 4766. (doi:10.1038/srep04766)

62. Hemelrijk CK, Hildenbrandt H, Reinders J, Stamhuis EJ. 2010 Emergence of Oblong School Shape: Models and Empirical Data of Fish. *Ethology* **116**, 1099–1112. (doi:10.1111/j.1439-0310.2010.01818.x)

63. Hemelrijk CK, Hildenbrandt H. 2008 Self-organized shape and frontal density of fish schools. *Ethology* **114**, 245–254. (doi:10.1111/j.1439-0310.2007.01459.x)

64. Kent MIA, Lukeman R, Lizier JT, Ward AJW. 2019 Speed-mediated properties of

schooling. *R. Soc. Open Sci.* **6**, 181482. (doi:10.1098/rsos.181482)

65. Tobalske BW. 2007 Biomechanics of bird flight. *J. Exp. Biol.* **210**, 3135–3146. (doi:10.1242/jeb.000273)

66. Tobalske BW, Hedrick TL, Dial KP, Biewener AA. 2003 Comparative power curves in bird flight. *Nature* **421**, 363–366. (doi:10.1038/nature01284)

67. Röell A. 1978 Social behaviour of the jackdaw, Corvus monedula , in relation to its niche. *Behaviour* **64**, 1–124.

68. Jolles JW, King AJ, Manica A, Thornton A. 2013 Heterogeneous structure in mixed-species corvid flocks in flight. *Anim. Behav.* **85**, 743–750. (doi:10.1016/j.anbehav.2013.01.015)

69. Franks NR, Richardson T. 2006 Teaching in tandem-running ants. *Nature* **439**, 153. (doi:10.1038/439153a)

70. Buhl J, Sword GA, Simpson SJ. 2012 Using field data to test locust migratory band collective movement models. *Interface Focus* **2**, 757–763. (doi:10.1098/rsfs.2012.0024)

71. Herbert-Read JE, Perna A, Mann RP, Schaerf TM, Sumpter DJT, Ward AJW. 2011 Inferring the rules of interaction of shoaling fish. *Proc. Natl. Acad. Sci.* **108**, 18726–18731. (doi:10.1073/pnas.1109355108)

72. Torney CJ, Lamont M, Debell L, Angohiatok RJ, Leclerc LM, Berdahl AM. 2018 Inferring the rules of social interaction in migrating caribou. *Philos. Trans. R. Soc. B Biol. Sci.* **373**. (doi:10.1098/rstb.2017.0385)

73. Maeng JS, Park JH, Jang SM, Han SY. 2013 A modeling approach to energy savings of flying Canada geese using computational fluid dynamics. *J. Theor. Biol.* **320**, 76–85. (doi:10.1016/j.jtbi.2012.11.032)

74. Iriarte-Diaz J, Swartz SM. 2008 Kinematics of slow turn maneuvering in the fruit bat Cynopterus brachyotis. *J. Exp. Biol.* **211**, 3478–3489. (doi:10.1242/jeb.017590)

75. Ros IG, Bassman LC, Badger MA, Pierson AN, Biewener AA. 2011 Pigeons steer like

549 helicopters and generate down- and upstroke lift during low speed turns. *Proc. Natl. Acad.*
550 *Sci.* **108**, 19990–19995. (doi:10.1073/pnas.1107519108)
551 76. Ling H, McIvor G, van der Vaart K, Vaughan R, Thornton A, Ouellette N. Data from: Local
552 interactions and their group-level consequences in flocking jackdaws. Dryad Digital
553 Repository. (doi: 10.5061/dryad.kb8js06)
554
555

Event	Total number of birds	Trajectory length (s)	*NND* (m)	$\|\boldsymbol{v}\|$ (m/s)	v_3 (m/s)	a_{Wing} (m/s^2)	a_{Move} (m/s^2)
Isolated pairs	610	4.0 ± 2.0	2.6 ± 1.7	9.4 ± 2.8	−0.3 ± 1.5	−0.3 ± 3.5	−0.1 ± 1.6
Flock #1	338	2.4 ± 1.1	1.6 ± 0.9	13.6 ± 1.7	−0.9 ± 0.8	−2.7 ± 3.3	−0.7 ± 1.8
Flock #2	112	3.1 ± 1.0	1.7 ± 0.8	13.8 ± 0.5	−0.3 ± 0.6	−0.4 ± 0.8	1.5 ± 1.8
Flock #3	106	2.9 ± 1.4	1.7 ± 1.0	12.0 ± 0.7	−0.6 ± 0.7	−0.1 ± 1.1	0.8 ± 1.8
Flock #4	81	4.5 ± 1.0	2.9 ± 2.7	10.1 ± 1.0	−0.8 ± 0.8	−0.4 ± 2.1	−0.1 ± 1.4
Flock #5	31	2.0 ± 1.2	1.3± 0.6	15.2± 0.8	−1.4 ± 1.6	−2.1 ± 4.3	−1.2 ± 1.8
Flock #6	26	3.4 ± 1.0	2.9± 2.7	9.3± 0.3	0.6 ± 0.4	−1.0 ± 0.5	−0.6 ± 0.7

556
557 Table 1. Statistics of bird flight in isolated pairs and in groups. *NND* denotes the first nearest neighbour
558 distance, v_3 denotes the velocity in the gravity direction, a_{Wing} and a_{Move} are the accelerations in the wing
559 and movement directions respectively. The values provided in the table are the means and standard
560 deviations. Positive (negative) values of a_{Move} mean speeding up (slowing down), and positive (negative)
561 a_{Wing} implies turning right (left).
562
563

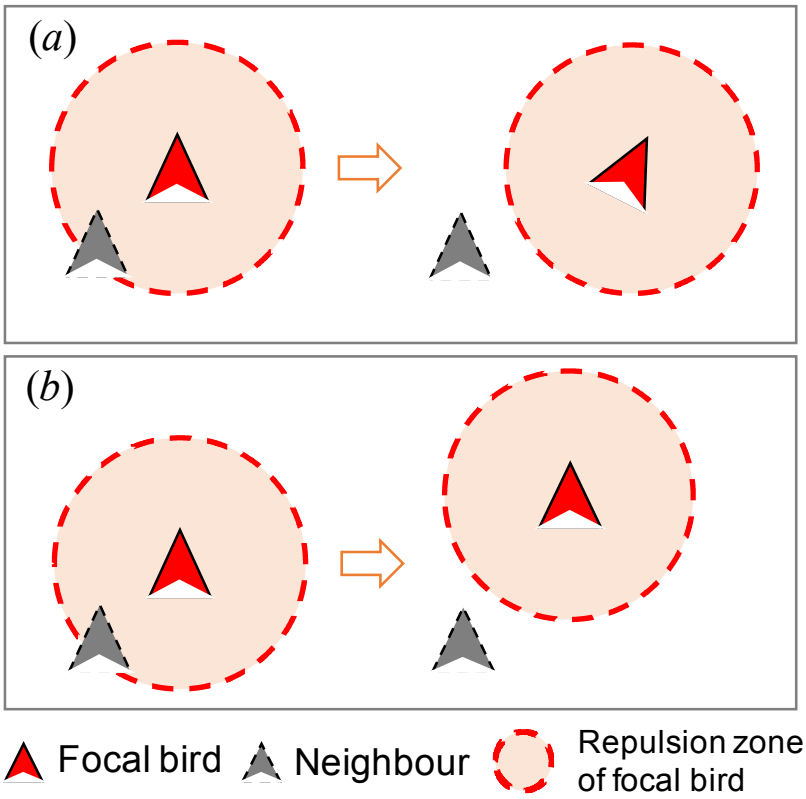

564
565 Figure 1. Anisotropic neighbour structure caused by repulsion: (a) turning-based repulsion creating a
566 side-by-side neighbour structure; (b) speeding-based repulsion forming a front-back neighbour
567 distribution.
568
569

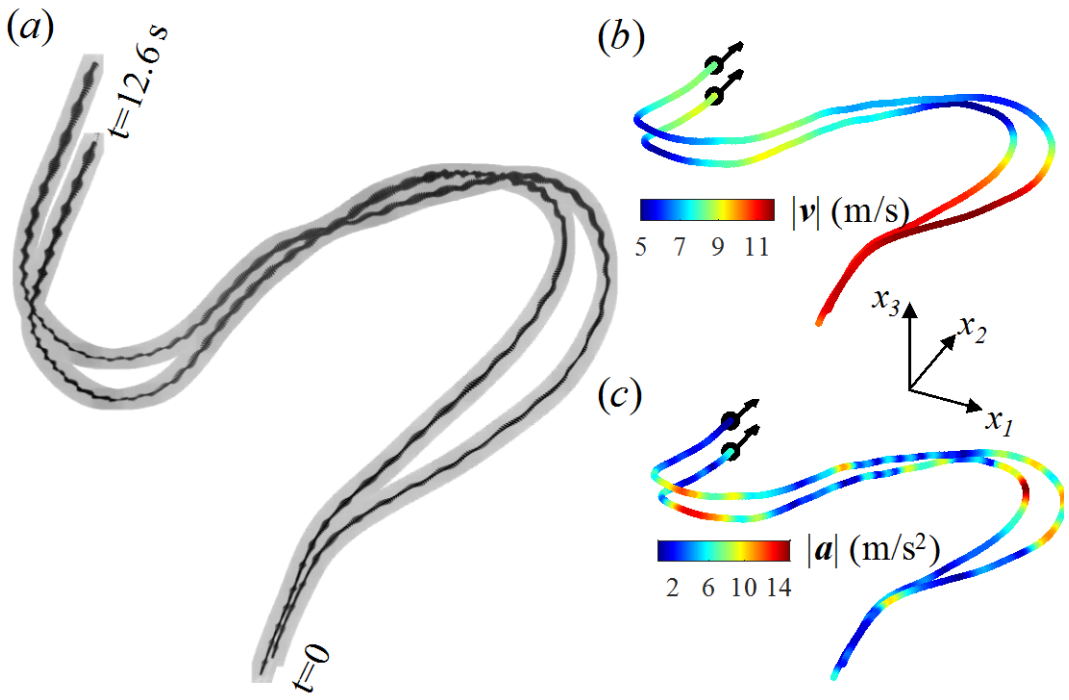

Figure 2. (a) Recorded images for isolated pairs. The time step between two consecutive images of the same bird is 1/60 s. (b-c) Reconstructed 3D trajectories for birds shown in (a) coloured by flight speed $|\boldsymbol{v}|$ (b) and acceleration $|\boldsymbol{a}|$ (c). More samples are provided in *electronic supplementary material figure S1*.

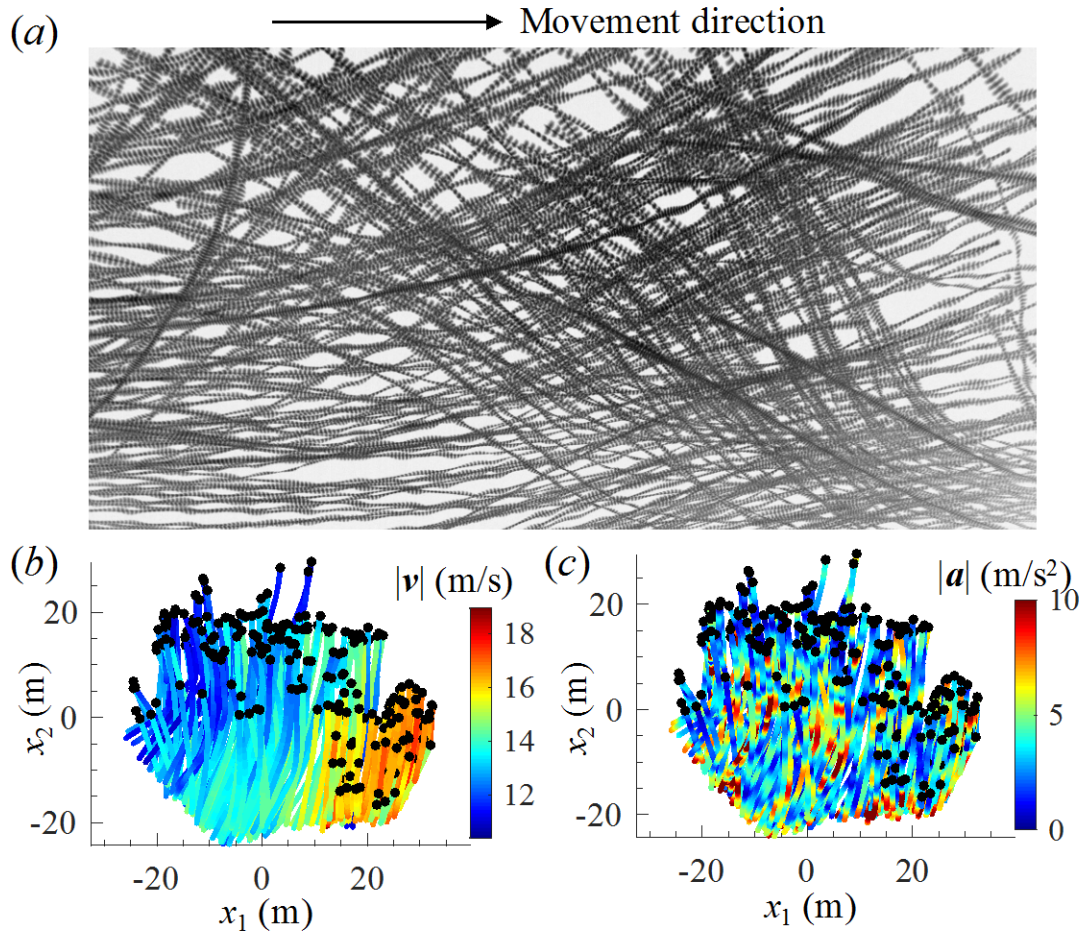

Figure 3. (a) Recorded images of birds in flock #1. The time step between two consecutive images of the same bird is 1/60 s. (b-c) Reconstructed 3D trajectories of flock #1 projected onto the horizontal plane coloured by $|\boldsymbol{v}|$ and $|\boldsymbol{a}|$. For flocks #2 to #6, see *electronic supplementary material figure S2*.

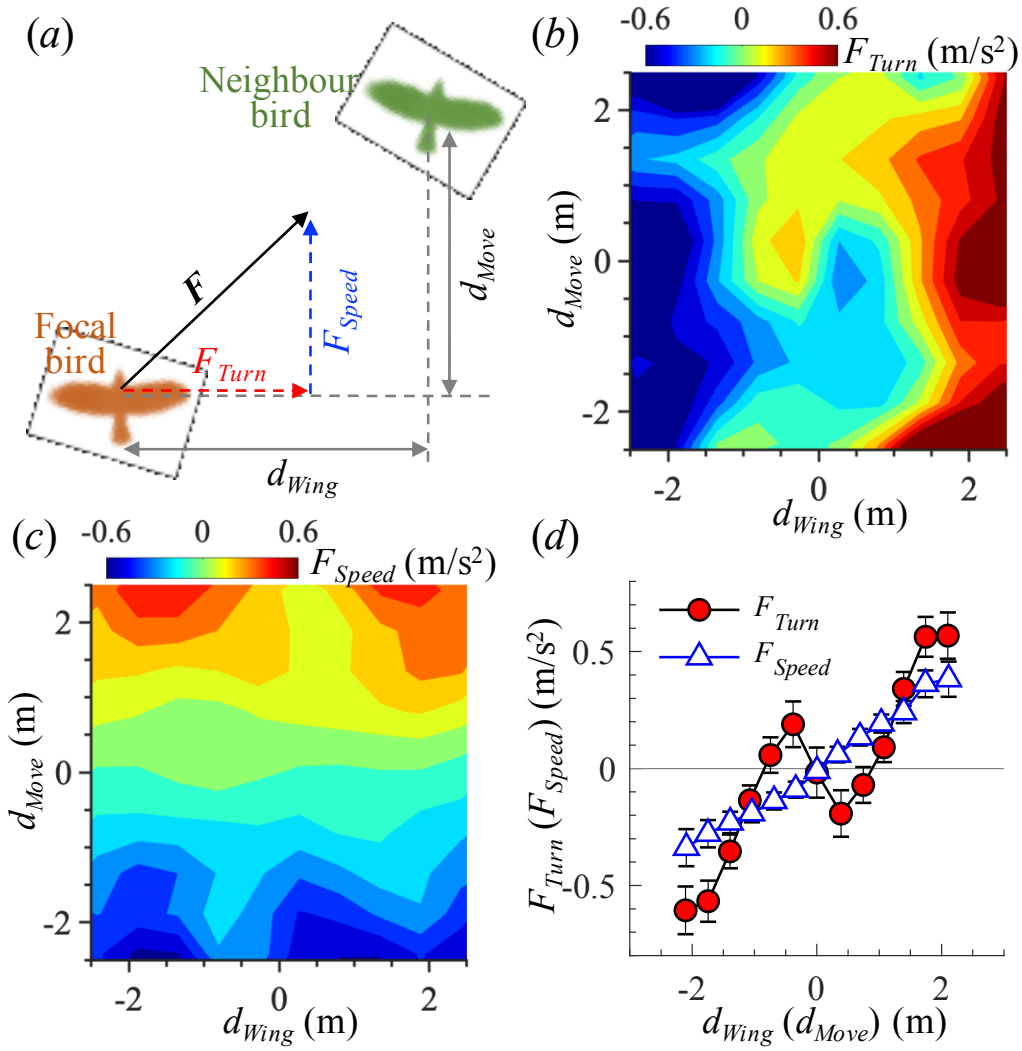

Figure 4. (a) Schematic of the measurement variables. We place the focal bird at the origin and measure the neighbour location denoted as (d_{Wing}, d_{Move}) and acceleration of focal bird relative to neighbour denoted as (F_{Turn}, F_{Speed}). (b-c) F_{Turn} (b) and F_{Speed} (c) as a function of d_{Wing} and d_{Move}. (d) F_{Turn} as a function of d_{Wing} (circles), and F_{Speed} as a function of d_{Move} (triangles). Data in (b-d) were obtained from 149,230 samples taken from 305 isolated pairs (see *electronic supplementary material*). 0.5 m/s² is much larger than average values of F_{Turn} and F_{Speed} for the 149,230 samples. Error bars are standard errors.

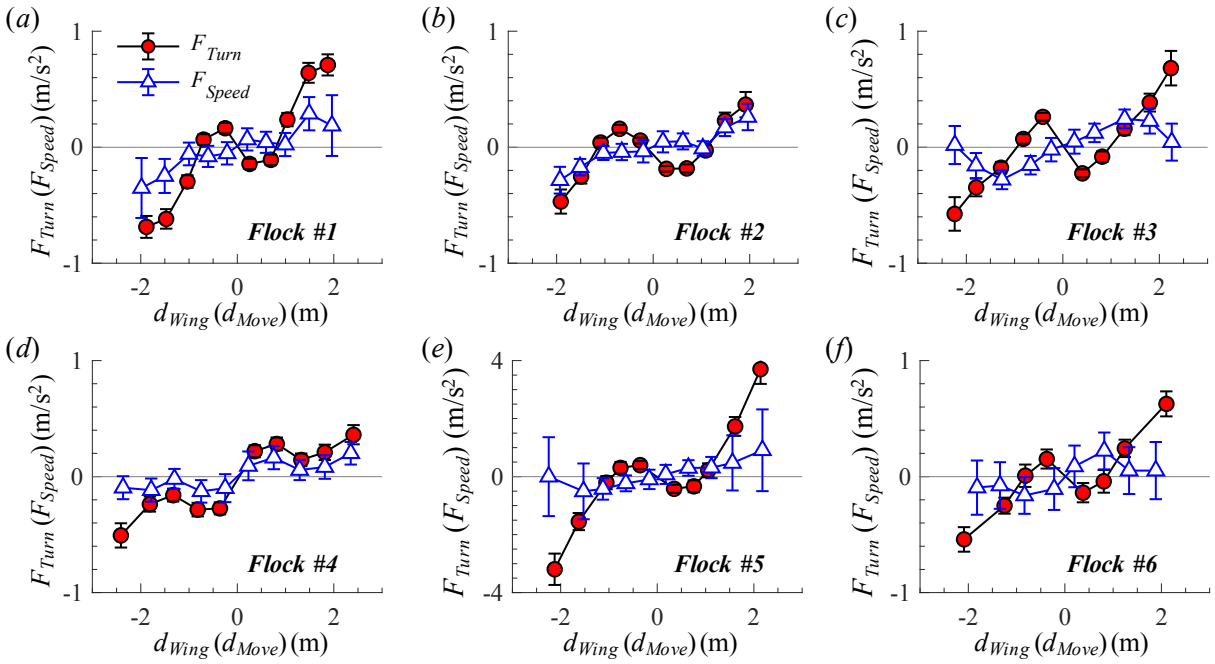

Figure 5. F_{Turn} as a function of d_{Wing} (circles), and F_{Speed} as a function of d_{Move} (triangles) for birds flying in large groups. Error bars are standard errors.

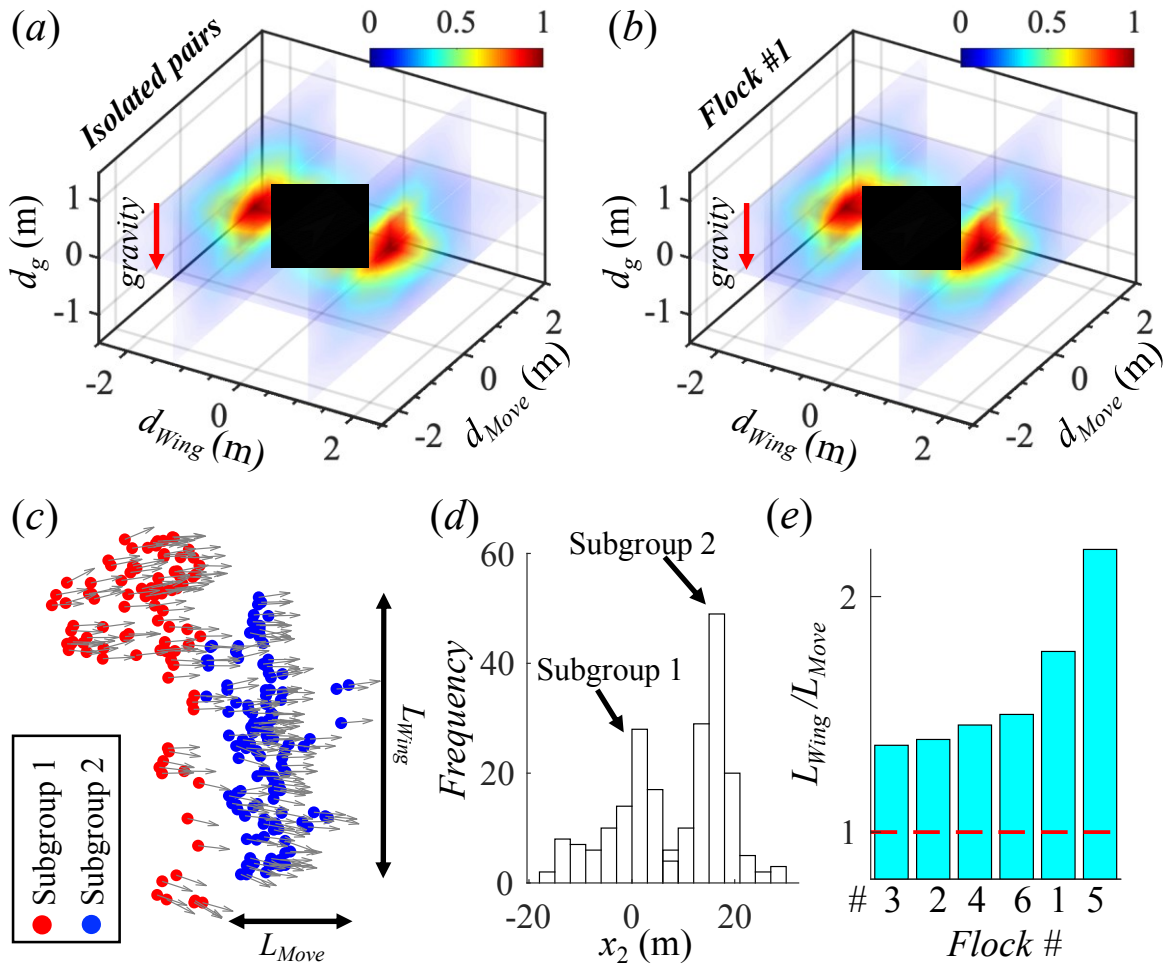

Figure 6. (a-b) Probability density distributions of the location of the first nearest neighbour bird in isolated pairs (a) and in a large flock (#1) (b). The focal bird is located at the origin. d_g is the distance in the gravity direction. (c) Distribution of bird locations (dots) projected on the horizontal plane for flock #1, showing two subgroups (one in red (grey) and one in blue (dark)) separated along the flight direction. The vectors are the movement directions of individual birds. (d) Corresponding histogram of bird positions along the flight direction (x_2). Data for flocks #2 to #6 can be found in *electronic supplementary material figure S4 and S5*. (e) Ratio of the subgroup size in the wing direction (L_{Wing}) to the subgroup size in the movement direction (L_{Move}).

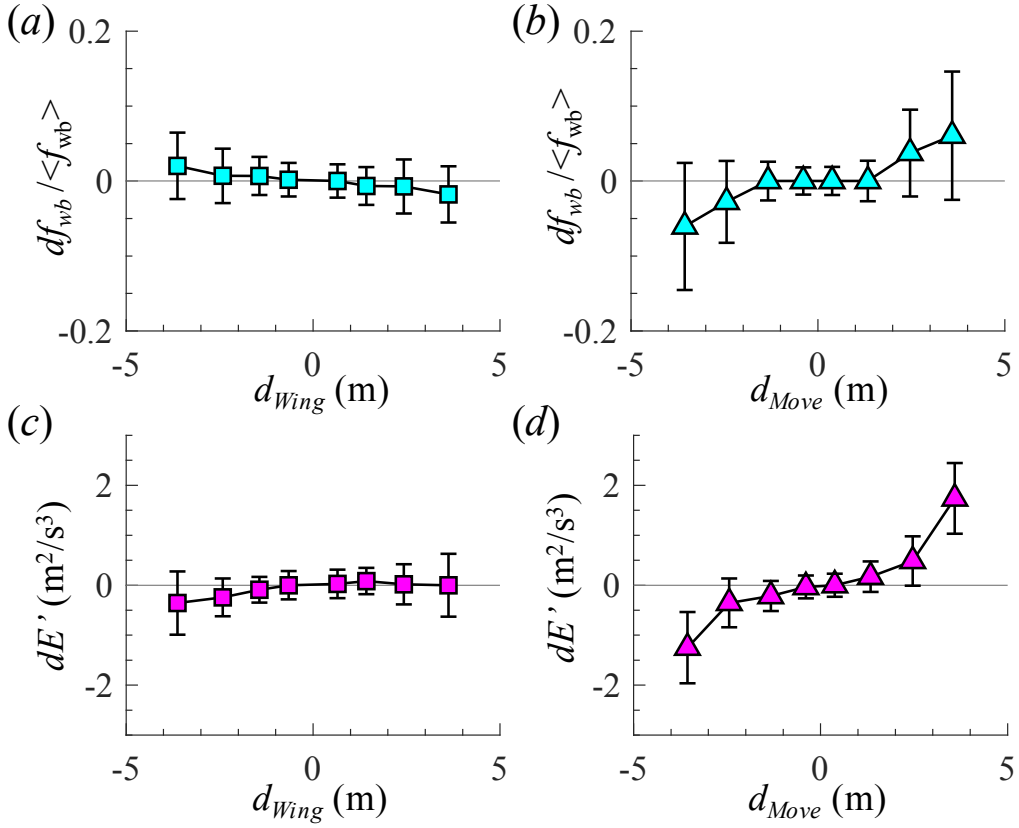

Figure 7. (a-b) df_{wb} as a function of d_{Wing} (a) and d_{Move} (b). (c-d) dE' as a function of d_{Wing} (c) and d_{Move} (d). Here, $df_{wb}>0$ indicates that focal birds flap their wings faster than their neighbours, and $dE'>0$ indicates that focal birds output more mechanical power than their neighbours. Results were obtained from 149,230 samples taken from 305 isolated pairs. Error bars are standard errors.